

X(2370) glueball-like particle productions in e^+e^- collisions at the BESIII energy and in pp collisions at the LHC energy with PACIAE model

Jian Cao,¹ Zhi-Lei She,^{2,*} Jin-Peng Zhang,¹ Jia-Hao Shi,¹ Zhi-Ying Qin,¹ Wen-Chao Zhang,^{1,†} Hua Zheng,¹ An-Ke Lei,³ Dai-Mei Zhou,^{3,‡} Yu-Liang Yan,⁴ and Ben-Hao Sa^{4,§}

¹*School of Physics and Information Technology, Shaanxi Normal University, Xi'an 710119, China*

²*Wuhan Textile University, Wuhan 430200, China*

³*Key Laboratory of Quark and Lepton Physics (MOE) and Institute of Particle Physics, Central China Normal University, Wuhan 430079, China*

⁴*China Institute of Atomic Energy, P. O. Box 275 (10), Beijing 102413, China*

(Dated: September 4, 2024)

Inspired by the BESIII newest observation of X(2370) glueball-like particle, we search its productions in both e^+e^- collisions at $\sqrt{s} = 4.95$ GeV and proton-proton (pp) collisions at $\sqrt{s} = 13$ TeV with a parton and hadron cascade model PACIAE. In this model, the final partonic state (FPS) and the final hadronic state (FHS) are consecutively simulated and recorded. The X(2370) glueball- or tetraquark-state is then, respectively, recombined by two gluons or four quarks $ss\bar{s}$ in the FPS using the quantum statistical mechanics inspired dynamically constrained phase-space coalescence (DCPC) model. The X(2370) molecular-state is recombined by the baryon-antibaryon of $\Lambda-\bar{\Lambda}$ or $\Sigma-\bar{\Sigma}$, or by three mesons of $\pi^+\pi^-\eta'$, $K^+K^-\eta'$, or $K_S^0K_S^0\eta'$ in the FHS using DCPC model. In both e^+e^- and pp collisions, significant discrepancies in the yields, the transverse momentum spectra and the rapidity distributions among the X(2370) glueball-, tetraquark-, and molecular-state are observed. These discrepancies are proposed as valuable criteria identifying the X(2370) different states from each other. Our results not only support the BESIII observation of glueball-like particle X(2370) production in e^+e^- collisions, but also serve as a prediction for the X(2370) production in pp collisions. We strongly suggest the experimental measurement of the X(2370) glueball-like particle production in pp collisions at the LHC energies.

I. INTRODUCTION

The constituent quark model [1, 2] has been the basic framework within which the conventional mesons and baryons could be understood. The non-Abelian property of quantum chromodynamics (QCD) permits the existence of new types of hadrons, such as the glueballs, hybrid states, hadronic molecular states and multi-quark states [3–5]. In particular, glueballs are unique particles which are bound states of gluons on their own, without any quarks involved. The Lattice QCD (LQCD) in the quenched approximation predicts that in the ground state the masses of the scalar, tensor and pseudo-scalar two-gluon glueballs are, respectively, around 1.5–1.7 GeV/ c^2 , 2.3–2.4 GeV/ c^2 and 2.3–2.6 GeV/ c^2 [6–10]. The hunting of glueballs is one of the important goals in hadron physics. A large number of experimental studies have been conducted in order to confirm their existence over the past four decades, mostly in radiative decays from J/ψ in e^+e^- collisions [11–13]. There are several glueball candidates, such as the scalar mesons $f_0(1500)$ and $f_0(1710)$, the tensor meson $f_2(2340)$, and the pseudo-scalar meson X(2370) [13]. Among them, the X(2370) is a good candidate for the 0^{-+} glueball, as its mass, production and decay properties are consistent with the

LQCD prediction [14].

The X(2370) was first observed in the $\pi^+\pi^-\eta'$ invariant mass distribution of the $J/\psi \rightarrow \gamma\pi^+\pi^-\eta'$ decay by the BESIII collaboration [14]. Later, it was confirmed by the collaboration in the combined measurement of $J/\psi \rightarrow \gamma K^+K^-\eta'$ and $J/\psi \rightarrow \gamma K_S^0K_S^0\eta'$ [15]. Recently, the spin-parity of the X(2370) was determined to be 0^{-+} for the first time in the decay $J/\psi \rightarrow \gamma K_S^0K_S^0\eta'$ [16]. The experimental observation stimulated a number of theoretical interpretations for the X(2370), such as the fourth radial excitation of η/η' [17, 18], the P -wave $ss\bar{s}$ tetraquark state [19], the light baryonium states $\Lambda-\bar{\Lambda}$ and $\Sigma-\bar{\Sigma}$ [20]. One of the intriguing explanations is that the X(2370) is a pseudoscalar glueball [10]. There are two possible compositions for the pseudoscalar glueball: two- or three-gluons [21]. The experimental result at BESIII is in favor of the X(2370) as the two-gluon glueball structure [16]. The X(2370) could not be a pseudoscalar glueball composed of three gluons, as the mass prediction from the quenched LQCD for this configuration is around 3.4–3.6 GeV/ c^2 [22, 23], which is much heavier than the mass of the X(2370) measured.

Apart from the radiative J/ψ decay in e^+e^- collisions, the proton-proton (pp) collisions are also theoretically suggested to search for glueballs [22]. In this paper, we carry out the investigation of the X(2370) productions in both e^+e^- collisions at the center-of-mass energy $\sqrt{s} = 4.95$ GeV and pp collisions at $\sqrt{s} = 13$ TeV with a parton and hadron cascade model PACIAE [24]. In the model, the final partonic state (FPS) and the final hadronic state (FHS) are consecutively simulated and recorded. There

* shezhilei@cug.edu.cn

† wenchao.zhang@snnu.edu.cn

‡ zhoudm@mail.ccnu.edu.cn

§ sabhliuym35@qq.com

are three scenarios considered for the configuration of the X(2370): the glueball-, tetraquark- and molecular-state. The glueball- and tetraquark-state are, respectively, produced by coalescing with two gluons and four quarks of $ss\bar{s}$ in the FPS using the quantum statistical mechanics inspired dynamically constrained phase-space coalescence (DCPC) model [25]. The molecular-state is generated by recombining the baryon-antibaryon ($B-\bar{B}$) of $\Lambda-\bar{\Lambda}$ or $\Sigma-\bar{\Sigma}$, or three mesons of $\pi^+\pi^-\eta'$, $K^+K^-\eta'$ or $K_S^0K_S^0\eta'$ in the FHS. The resulted X(2370) yields, rapidity (y) distributions, transverse momentum (p_T) single-differential distributions, as well as p_T and y double-differential distributions in both e^+e^- and pp collisions show significant discrepancies between the X(2370) different states. These discrepancies are proposed as valuable criteria identifying the X(2370) different states from each other. Our results not only support the BESIII observation of glueball-like particle X(2370) production in e^+e^- collisions, but also serve as a prediction for the X(2370) production in pp collisions. We strongly suggest the experimental measurement of the X(2370) glueball-like particle production in pp collisions at the LHC energies.

II. THE PACIAE AND DCPC MODELS

The PACIAE model is designed for the relativistic elementary collisions and nuclear collisions [26]. It is based on PYTHIA 6.4 code [27] but extended considering the partonic rescattering before hadronization and the hadronic rescattering after hadronization. It has been successfully applied in describing the hadron yields, p_T spectra and y distributions [24, 26, 28], the strangeness enhancement [29, 30], the nuclear modification factor [31, 32], the elliptic flow [33, 34], etc., in the high-energy particle and nuclear collisions. In this work, the latest version of PACIAE 3.0 [24] is used to simulate e^+e^- collisions at $\sqrt{s} = 4.95$ GeV and pp collisions at $\sqrt{s} = 13$ TeV. In PACIAE model, an e^+e^- or a pp collision is developed from the initial parton stage, to the parton rescattering stage, the hadronization, and the hadron rescattering stage. As an example, figure 1 shows a sketch of the physical routines in a high-energy pp collision.

In the first stage, both the e^+e^- and the pp collision is executed by PYTHIA [27] with temporarily switching off the string fragmentation. Thus an initial partonic state is available after the parton-parton hard scattering, the associated initial- and final-state QCD radiations, the strings broken down and the diquarks (anti-diquarks) splitted up. This partonic matter then undergoes parton rescatterings, where the leading order (LO) pQCD parton-parton scattering cross sections [35, 36] are employed. The final partonic state is generated after partonic rescattering. It consists of numerous quarks, anti-quarks and gluons with their four-coordinate and four-momentum. In the hadronization stage, the partonic

matter is converted into hadrons by the string fragmentation scheme [27]. The followed is then the hadronic rescattering resulting in a final hadronic state. It is composed of abundant hadrons with their four-coordinate and four-momentum. A sketch of the aforementioned processes in e^+e^- or pp collisions is presented in the left part of Fig. 2.

The DCPC model was proposed by us to study the light nuclei production in pp collisions at the LHC energies [25]. It has been successfully applied to calculate the yield of the exotic states such as the X(3872) [37–39], $Z_c^\pm(3900)$ [40], $P_c(4312)$, $P_c(4440)$, $P_c(4457)$ [41], and Ω_c^0 [42] after the transport model simulation. In DCPC model, the yield of N -particle cluster is estimated according to the quantum statistical mechanics [25, 43, 44] by

$$Y_{\text{cluster}} = \int \cdots \int_{E_1 \leq E \leq E_2} \frac{d\vec{q}_1 d\vec{p}_1 \cdots d\vec{q}_N d\vec{p}_N}{h^{3N}}, \quad (1)$$

where E_1 and E_2 are the cluster's lower and upper energy thresholds, \vec{q}_i and \vec{p}_i are the i th particle's three-coordinate and three-momentum, respectively. Therefore, the yield of the X(2370) two-gluon glueball-state, for instance, reads

$$Y_{\text{glueball}} = \frac{1}{2!} \int \int_{E_1 \leq E \leq E_2} \delta_{12} \frac{d\vec{q}_1 d\vec{p}_1 d\vec{q}_2 d\vec{p}_2}{h^6}, \quad (2)$$

where the factor $1/2!$ is introduced as gluons are identical particles. In the above equation δ_{12} is expressed as

$$\delta_{12} = \begin{cases} 1, & \text{if } 1 \equiv g, 2 \equiv g, R_i \leq R_0, \text{ and} \\ & m_0 - \Delta m \leq m_{\text{inv}} \leq m_0 + \Delta m, \\ 0, & \text{otherwise} \end{cases}, \quad (3)$$

where m_0 refers to the mass of the X(2370), Δm is the mass uncertainty (a free parameter) which is estimated as the half decay width of the X(2370) [16]. R_0 and R_i are, respectively, the radius of the glueball (a free parameter) and the relative distance between the component particle i and the center of mass of the glueball. R_0 is set to be 1 fm as gluons are point-like particles. The invariant mass, m_{inv} , is calculated as $m_{\text{inv}} = \sqrt{(E_1 + E_2)^2 - (\vec{p}_1 + \vec{p}_2)^2}$, where $E_{1,2}$ and $\vec{p}_{1,2}$ are, respectively, the energy and momentum of the selected gluons 1 and 2.

The yield of the X(2370) tetraquark- or molecular-state can be evaluated in a similar way with different parameters. The parameters of mass uncertainty and radius are given in Table I.

To generate the X(2370) two-gluon glueball-state, a component particle (gluon) list based on the parton list in FPS is constructed first. Two loops over i and j cycling through all gluons in the list are implemented. If i and j are two different gluons and they satisfy the constraints in Eq. (3), the combination of these two gluons is then deemed as an X(2370) glueball-state. The gluon list is then updated by removing the used gluons. A new two-layer cycle is executed on the updated list. Repeat these steps until the empty of the list or the rest in the

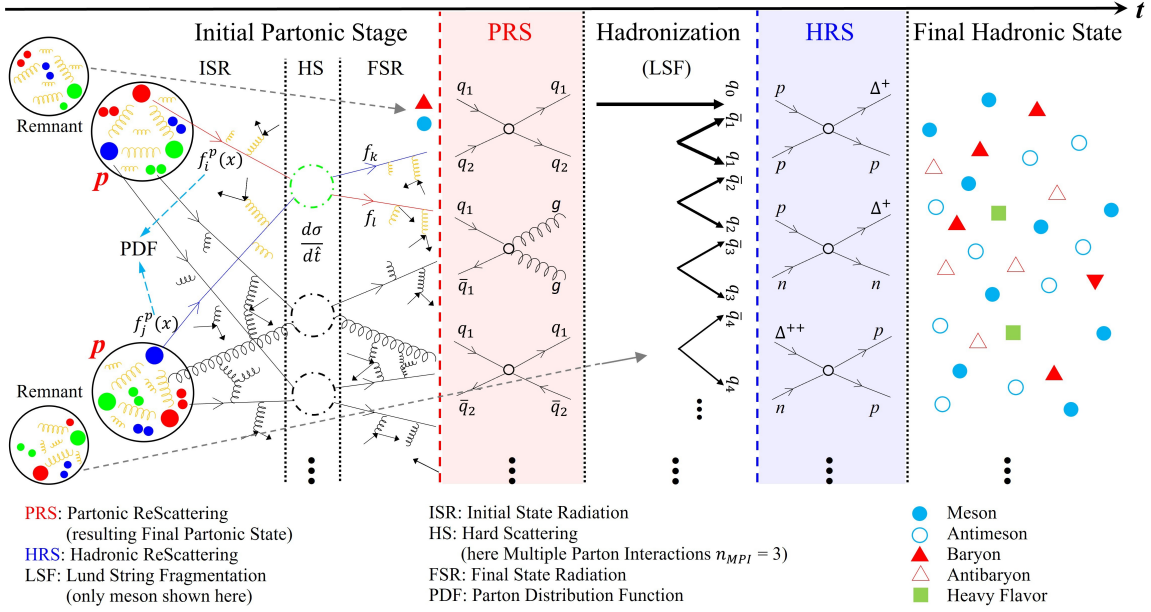


FIG. 1. A sketch of the physical routines in high energy pp collisions.

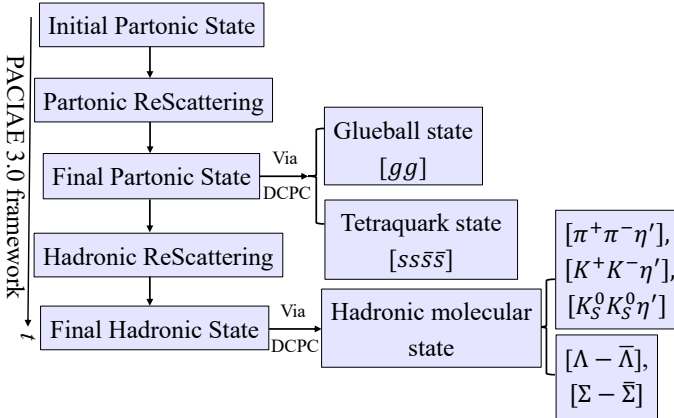


FIG. 2. A sketch of the X(2370) glueball-, tetraquark- and molecular-state productions in e^+e^- collisions at $\sqrt{s}=4.95$ GeV or in pp collisions at $\sqrt{s}=13$ TeV with the PACIAE+DCPC model.

list is unable to generate an X(2370) glueball-state. The production of the X(2370) tetraquark-state is done in a similar way. The procedure to generate the molecular-state composed of three mesons is a little bit different. A component particle list of π^+ , π^- , K^+ , K^- , K_S^0 , and η' based on the hadron list in the FHS is constructed. Three loops cycling through all component particles are implemented. Each combination, if it is $\pi^+ + \pi^- + \eta'$, $K^+ + K^- + \eta'$, or $K_S^0 + K_S^0 + \eta'$ and satisfies the constraints like those in Eq. (3) without the extra factor $1/2!$, is assumed to be an X(2370) molecular-state. The generation of the X(2370) molecular-state composed of baryon-antibaryon is performed in a similar way.

TABLE I. The parameters of mass uncertainty and radius for the X(2370) glueball-, tetraquark- and molecular-state.

	glueball	tetraquark	molecular $B-\bar{B}$	3 mesons
Δm (MeV/c ²)	94	94	94	94
R_0 (fm)	1.0	1.0	1.0-2.0 ^a	1.0-2.0 ^b

^a The R_0 upper bound of the $B-\bar{B}$ molecular-state is taken as the radius summation of the baryon and antibaryon.

^b The R_0 upper bound of the 3-meson molecular-state is assumed to be the same as that of the $B-\bar{B}$ molecular-state.

III. RESULTS AND DISCUSSIONS

The PACIAE 3.0 model is used to simulate the X(2370) productions in both e^+e^- collisions at $\sqrt{s}=4.95$ GeV and pp collisions at $\sqrt{s}=13$ TeV. For e^+e^- collisions, default parameters are utilized, as so far there are no experimental yields of pions and kaons available to tune the parameters. For pp collisions, the model parameters are chosen as the default values, except for PARP(31), PARJ(1), PARJ(2) and PARJ(42). PARP(31) is a common K factor multiplying the differential cross section of hard parton-parton scattering processes. PARJ(1) represents the suppression of diquark-antidiquark pair production in string-breaking processes, compared with quark-antiquark pair production. PARJ(2) denotes the suppression of s quark pair production relative to the u or d pair production. PARJ(42) gives the parameter b in Lund fragmentation function. For more details, we refer to Ref. [27]. These parameters, as listed in Table II, are

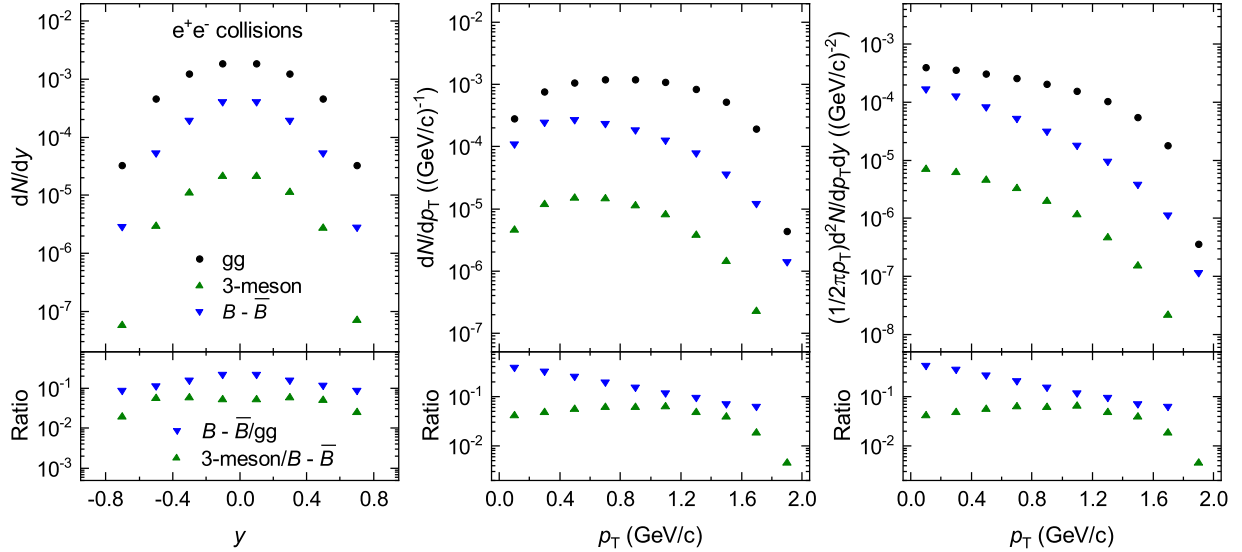


FIG. 3. Upper panes: the simulated y and p_T single-differential distributions, as well as p_T and y double-differential distributions of the X(2370) glueball-state, $B\text{-}\bar{B}$ and 3-meson molecular-state in e^+e^- collisions at $\sqrt{s} = 4.95$ GeV. Lower panels: the ratio between two distributions denoted by legend.

fixed by fitting to the experimental yields of $\pi^+ + \pi^-$, $K^+ + K^-$, K_S^0 , and $\Lambda + \bar{\Lambda}$ in the mid-rapidity region [45]. The fitted results of those yields and the corresponding experimental data are given in Table III.

TABLE II. The PACIAE model parameters of PARP(31), PARJ(1), PARJ(2) and PARJ(42) are fixed by fitting the $\pi^+ + \pi^-$, $K^+ + K^-$, K_S^0 , and $\Lambda + \bar{\Lambda}$ yields measured in the mid-rapidity region of pp collisions at $\sqrt{s} = 13$ TeV.

PARP(31)	PARJ(1)	PARJ(2)	PARJ(42)
1.0	0.18	0.42	1.35

TABLE III. The PACIAE model simulated yields of $\pi^+ + \pi^-$, $K^+ + K^-$, K_S^0 , and $\Lambda + \bar{\Lambda}$ are compared with the ALICE data in pp collisions at $\sqrt{s} = 13$ TeV [45].

	$\pi^+ + \pi^-$	$K^+ + K^-$	K_S^0	$\Lambda + \bar{\Lambda}$
Exp.	4.78 ± 0.24	0.62 ± 0.03	0.32 ± 0.01	0.18 ± 0.01
PACIAE	4.83	0.65	0.32	0.18

Using the PACIAE model, we have generated 800 million e^+e^- collisions with the default parameters and 100 million pp collision events with the parameters listed in Table II. As shown in the right part of Fig. 2, the X(2370) glueball- and tetraquark-state are generated, respectively, by the recombination of two gluons and of four quarks ($ss\bar{s}\bar{s}$) in the FPS using the DCPC model. The X(2370) molecular-state is hadronized by the coalescence of baryon-antibaryon ($\Lambda\text{-}\bar{\Lambda}$ or $\Sigma\text{-}\bar{\Sigma}$) or of three

TABLE IV. The PACIAE+DCPC model simulated yields of the X(2370) glueball-, tetraquark-, and molecular-state in e^+e^- collisions at $\sqrt{s} = 4.95$ GeV and in pp collision at $\sqrt{s} = 13$ TeV.

	glueball	tetraquark	molecular	
			$B\text{-}\bar{B}$ ^a	3 mesons ^b
e^+e^-	1.42×10^{-3}	—	2.63×10^{-4}	1.40×10^{-5}
pp	1.50	2.63×10^{-4}	4.12×10^{-2}	3.13×10^{-3}

^a $B\text{-}\bar{B}$ refers to the summation over the yields of $\Lambda\text{-}\bar{\Lambda}$ and $\Sigma\text{-}\bar{\Sigma}$.

^b 3-meson refers to the summation over the yields of $\pi^+\pi^-\eta'$, $K^+K^-\eta'$ and $K_S^0K_S^0\eta'$.

mesons ($\pi^+\pi^-\eta'$, $K^+K^-\eta'$ or $K_S^0K_S^0\eta'$) in the FHS. Their yields are given in Table IV. The yield of the X(2370) tetraquark-state in e^+e^- collisions is not available, as at the BESIII energy it is too tiny to be observed. Both the X(2370) glueball- and molecular-state successful generations definitely support the BESIII latest observation of glueball-like particle X(2370) productions in the e^+e^- collisions.

The particle y and p_T single-differential distributions, as well as the p_T and y double-differential distributions of the X(2370) glueball-state (black circles), $B\text{-}\bar{B}$ (blue triangles-down) and 3-meson (green triangles-up) molecular-state in e^+e^- collisions at $\sqrt{s} = 4.95$ GeV are calculated and shown in Fig. 3. Significant discrepancies between the X(2370) different states are observed in all the above distributions. Thus they can serve as criteria to distinguish the X(2370) different states from each other. The origin of the different behavior of the three

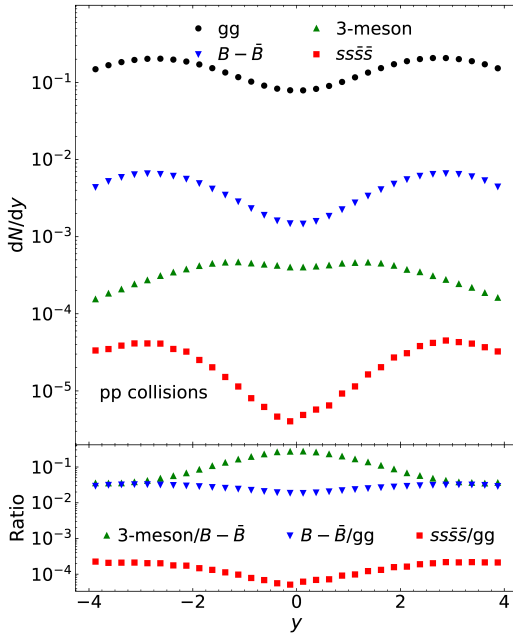


FIG. 4. Upper panel: the simulated y single-differential distributions of the X(2370) glueball-state, tetraquark-state, $B-\bar{B}$ and 3-meson molecular-state in pp collisions at $\sqrt{s}=13$ TeV. Lower legend

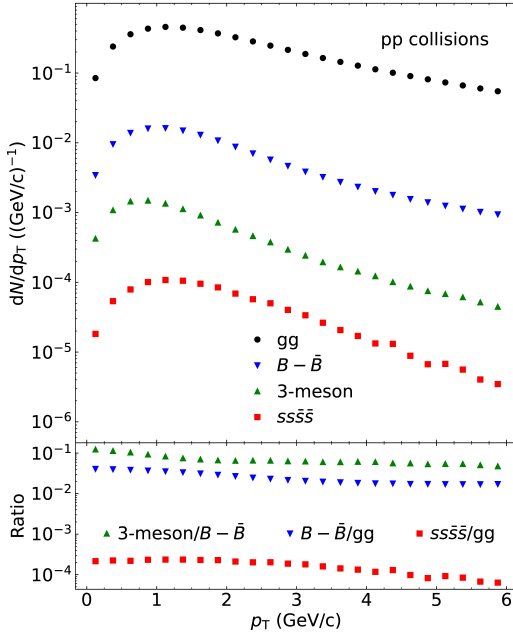


FIG. 5. The same as in Fig. 4, but for the p_T single-differential distributions.

states is linked to the nature of the X(2370), not to the structure of the model, as both our model and a multi-phase transport model (AMPT) [46] show that the rapidity (and p_T) distributions of the X(3872) tetraquark- and molecular-state are different in high energy nuclear collisions [39, 47].

The upper panels in Figs. 4 and 5 show, respectively, the simulated y and p_T single-differential distributions in pp collisions at $\sqrt{s}=13$ TeV for the X(2370) glueball-state (black circles), tetraquark-state (red squares), $B-\bar{B}$ (blue triangles-down) and 3-meson (green triangles-up) molecular-state. The upper and lower panels in Fig. 6 present the simulated p_T and y double-differential distributions for the X(2370) different states in pp collisions at $\sqrt{s}=13$ TeV in the mid- and forward-rapidity regions, respectively. Obvious discrepancies are also observed among the X(2370) different states both in y and p_T single-differential distributions, as well as in the p_T and y double-differential distributions. Either of them could serve :
ferent

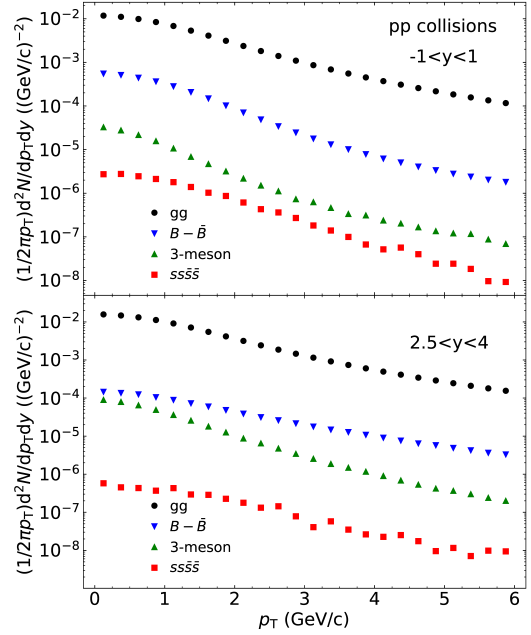


FIG. 6. The simulated p_T and y double-differential distributions of the X(2370) glueball-state, tetraquark-state, $B-\bar{B}$ and 3-meson molecular-state at mid- and forward-rapidity in pp collisions at $\sqrt{s}=13$ TeV.

Finally, the same as done in Ref. [39], we explore the temperature evolution in pp collisions. The temperature evolution in e^+e^- collisions is not considered, as the collision energy is low and the partonic matter is not thermalized. With the simulated $u + \bar{u} + d + \bar{d} + g$ in the FPS and $\pi^+ + \pi^-$ in FHS, the Shannon entropies of the partonic matter (PM) and hadronic matter (HM) are, respectively, calculated by [48]

$$\mathcal{H} = - \int_0^\infty (\text{TMD}/I_0) \ln[\text{TMD}/I_0] dp_T, \quad (4)$$

with TMD and I_0 being to the p_T distribution and its first moment, respectively. The temperatures T of the PM and HM are then determined by [48]

$$\mathcal{H} = \frac{m}{m-1} + \ln\left(\frac{m}{m-1}\right) + \ln(T), \quad (5)$$

where m is extrapolated from its energy dependence, $m(\sqrt{s}) = a_m(\sqrt{s/s_0})^{c_m}$, with $a_m = 8.45$, $c_m = -0.082$, $\sqrt{s_0} = 1$ GeV. The extracted results are $T_{\text{HM}} = T_{\text{molecular}} = 160$ MeV and $T_{\text{QM}} = T_{\text{glueball/tetraquark}} = 232$ MeV, which are independent of the DCPC model. The temperature of the HM in pp collisions at $\sqrt{s} = 13$ TeV (160 MeV) is lower than that in pp collisions at $\sqrt{s} = 2.76$ TeV (180 MeV) [39]. This is due to the different hadronization mechanisms utilized. In this work, the string fragmentation scheme [27] is applied while in Ref. [39] the coalescence model [24] is implemented.

Based on the BESIII newest observation of the glueball-like particle X(2370) and our simulated results in e^+e^- and pp collisions, we strongly suggest that the ALICE and LHCb collaborations, respectively, measure the X(2370) production in pp collisions at the LHC energy in the mid-rapidity and forward-rapidity regions. It will be lighting up the determination of the X(2370) nature.

It is worth extending the investigation to Pb-Pb collisions at $\sqrt{s_{\text{NN}}} = 2.76$ and 5.02 TeV. The ultra-relativistic heavy-ion collisions might be an ideal tool to produce glueball as the existence of quark-gluon plasma (QGP) provides a large amount of thermal gluons [22]. In this gluon-rich environment, the gluons can form glue-

balls. With the QGP cooling further and freezing-out into hadronic matter, these glueballs might decay into light hadrons, which will give rise to signatures of their existence.

ACKNOWLEDGMENTS

We would like to thank San Jin, Yan-Ping Huang, Zhi-Qing Liu and Li-Lin Zhu for the valuable discussions. This work is supported by the National Natural Science Foundation of China under grant Nos. 11447024, 11505108 and 12375135, and by the 111 project of the foreign expert bureau of China. Y.L.Y. acknowledges the financial support from Key Laboratory of Quark and Lepton Physics in Central China Normal University under grant No. QLPL201805 and the Continuous Basic Scientific Research Project (No, WDJC-2019-13). W.C.Z. is supported by the Natural Science Basic Research Plan in Shaanxi Province of China (No. 2023-JCYB-012). H.Z. acknowledges the financial support from Key Laboratory of Quark and Lepton Physics in Central China Normal University under grant No. QLPL2024P01.

-
- [1] M. Gell-Mann, Phys. Lett. **8**, 214 (1964).
[2] G. Zweig, Report No. CERN-TH-401.
[3] C. Amsler and N.A. Tornqvist, Phys. Rep. **389**, 61 (2004).
[4] E. Klempt and A.Zaitsev, Phys. Rep. **454**, 1 (2007).
[5] V. Crede and C. Meyer, Prog. Part. Nucl. Phys. **63**, 74 (2009).
[6] G.S. Bali, et al., Phys. Lett. B **309**, 378 (1993).
[7] C.J. Morningstar and M. J. Peardon, Phys. Rev. D **60**, 034509 (1999).
[8] Y. Chen et al., Phys. Rev. D **73**, 014516 (2006).
[9] A. Irving, B. Lucini, C. McNeile, A. Rago, C. Richards and E. Rinaldi, J. High Energy Phys. **10**, 170 (2012).
[10] L.-C. Gui, J.-M. Dong, Y. Chen and Y.-B. Yang, Phys. Rev. D **100**, 054511 (2019).
[11] E. Klempt and A. Zaitsev, Phys. Rept., **454**, 1–202 (2007).
[12] V. Crede and C.A. Meyer, Prog. Part. Nucl. Phys., **63**, 74–116 (2009).
[13] H.-X. Chen, W. Chen, X. Liu, Y.-R. Liu and S.-L. Zhu, Rep. Prog. Phys. **86**, 026201 (2023).
[14] M. Ablikim et al. (BESIII Collaboration), Phys. Rev. Lett. **106**, 072002 (2011).
[15] M. Ablikim et al. (BESIII Collaboration), Eur. Phys. J. C **80**, 746 (2020).
[16] M. Ablikim et al. (BESIII Collaboration), Phys. Rev. Lett. **132**, 181901 (2024).
[17] J.-S. Yu, Z.-F. Sun, X. Liu and Q. Zhao, Phys. Rev. D **83**, 114007 (2011).
[18] L.-M. Wang, Q.-S. Zhou, C.-Q. Pang and X. Liu, Phys. Rev. D **102**, 114034 (2020).
[19] N. Su and H.-X. Chen, Phys. Rev. D **106**, 014023 (2022).
[20] B.-D. Wan, S.-Q. Zhang and C.-F. Qiao, Phys. Rev. D **105**, 014016 (2022).
[21] H.-X. Chen, W. Chen and S.-L. Zhu, Phys. Rev. D **104**, 094050 (2021).
[22] V. Mathieu, N. Kochelev and V. Vento, Int. J. Mod. Phys. E **18**, 1-49 (2009).
[23] H. B. Meyer, arXiv:hep-lat/0508002
[24] A.-K. Lei et al., Phys. Rev. C **108**, 064909 (2023).
[25] Y.-L. Yan, G. Chen, X.-M. Li, D.-M. Zhou, M.-J. Wang, S.-Y. Hu, L. Ye and B.-H. Sa, Phys. Rev. C **85**, 024907 (2012).
[26] B.-H. Sa, D.-M. Zhou, Y.-L. Yan, X.-M. Li, S.-Q. Feng, B.-G. Dong and X. Cai, Comput. Phys. Commun. **183**, 333–346 (2012).
[27] T. Sjöstrand, S. Mrenna and P. Skands, J. High Energy Phys. **05**, 026 (2006).
[28] K.-F. Ye, Q. Wang, J.-H. Shi, Z.-Y. Qin, W.-C. Zhang, A.-K. Lei, Z.-L. She, Y.-L. Yan and B.-H. Sa, Phys. Rev. C **109**, 035201 (2024).
[29] L. Zheng, D.-M. Zhou, Z.-B. Yin, Y.-L. Yan, G. Chen, X. Cai and B.-H. Sa, Phys. Rev. C **98**, 034917 (2018).
[30] D.-M. Zhou, L. Zheng, Y.-L. Yan, Z.-H. Song, G. Chen, X.-M. Li, X. Cai and B.-H. Sa, Phys. Rev. C **102**, 044903 (2020).
[31] A.-K. Lei, D.-M. Zhou, Y.-L. Yan, D.-J. Wang, X.-M. Li, G. Chen, X. Cai and B.-H. Sa, Phys. Rev. C **107**, 054914 (2023).
[32] F.-X. Liu, Z.-L. She, H.-G. Xu, D.-M. Zhou, G. Chen and B.-H. Sa, Sci. Rep. **12**, 1772 (2022).
[33] B.-H. Sa, D.-M. Zhou, Y.-L. Yan, B.-G. Dong and X. Cai, Comput. Phys. Commun. **184**, 1476–1479 (2013).
[34] B.-H. Sa, D.-M. Zhou, Y.-L. Yan, Y. Cheng, B.-G. Dong and X. Cai, Phys. Lett. B **731**, 87–91 (2014).
[35] B.L. Combridge, J. Kripfganz and J. Ranft., Phys. Lett. B **70**, 234 (1977).

- [36] R.D. Field, Applications off Perturbative QCD, Addison-Wesley Publishing Company, 1989.
- [37] H.-G. Xu, Z.-L. She, D.-M. Zhou, L. Zheng, X.-L. Kang, G. Chen and B.-H. S, Eur. Phys. J. C **81**, 784 (2021).
- [38] C.-T. Wu, Z.-L. She, X.-Y. Peng, X.-L. Kang, H.-G. Xu, D.-M. Zhou, G. Chen and B.-H. Sa, Phys. Rev. D **107**, 114022 (2023).
- [39] Z.-L. She et al., Phys. Rev. C **110**, 014910 (2024).
- [40] Z. Zhang, L. Zheng, G. Chen, H.-G. Xu, D.-M. Zhou, Y.-L. Yan, B.-H. Sa, Eur. Phys. J. C **81**, 198 (2021).
- [41] C.-H. Chen, Y.-L. Xie, H.-g. Xu, Z. Zhang, D.-M. Zhou, Z.-L. She and G. Chen, Phys. Rev. D. **105**, 054013 (2022).
- [42] H.-G. Xu, G. Chen, Y.-L. Yan, D.-M. Zhou, L. Zheng, Y.-L. Xie, Z.-L. She and B.-H. Sa, Phys. Rev. C **102**, 054319 (2020).
- [43] K. Stowe, An Introduction to Thermodynamics and Statistical Mechanics (Cambridge University, Cambridge, England, 2007).
- [44] R. Kubo, H. Ichimura, T. Usui and N. Hashizume, Statistical Mechanics: An Advanced Course with Problems and Solutions (North-Holland, Amsterdam, 1965).
- [45] S. Acharya et al. (ALICE Collaboration), Eur. Phys. J. C **81**, 256 (2021).
- [46] Z.-W. Lin, C.M. Ko, B.-A. Li, B. Zhang, and S. Pal, Phys. Rev. C **72**, 064901 (2005).
- [47] H. Zhang, J.-F. Liao, E.-K. Wang, Q. Wang, and H.-X. Xing, Phys. Rev. Lett. **126**, 012301 (2021).
- [48] D. Rosales Herrera, J.R. Alvarado García, A. Fernández Téllez, J.E. Ramírez, and C. Pajares, Phys. Rev. C **109**, 034915 (2024).